Suppression of the 0-π transition in a Josephson junction with parallel double-quantum-dot barriers

Guang-Yu Yi,[1] Xiao-Qi Wang,[1] Cui Jiang,[2] and Wei-Jiang Gong[1,*]
[1]*College of Sciences, Northeastern University, Shenyang 110819, China*
[2]*Basic Department, Shenyang Institute of Engineering, Shenyang 110136, China*

(Received 17 November 2017; revised manuscript received 11 June 2018; published 31 July 2018)

With the help of the numerical renormalization group method, we theoretically investigate the Josephson phase transition in a parallel junction with one quantum dot embedded in each arm. It is found that in the cases of appropriate dot levels and symmetrical dot-superconductor couplings, the Josephson phase transition will be suppressed. This is manifested as the fact that with the enhancement of the electron correlation, the supercurrent only arrives at its π' phase but cannot enter its π phase. Moreover, when the dot levels are detuned, one π'-phase island appears in the phase diagram. Such a result is attributed to the interplay among the Kondo effect, RKKY effect, and the Cooper pairing correlation. We believe that this work can be helpful in understanding the special roles of the correlation mechanisms of the parallel junction in driving the Josephson phase transition.

DOI: 10.1103/PhysRevB.98.035438

I. INTRODUCTION

The successful fabrication of quantum dots (QDs) allows scientists to investigate the conventional electron correlation in the mesoscopic circuits, due to their strong Coulomb repulsion and shiftable levels. It has been found that the Kondo effect, the most typical electron correlation, indeed affects electron tunneling [1–3]. Moreover, when one QD is introduced in a Josephson junction, the strong electron interaction drives the well-known Josephson phase transition [4–7]. If the Kondo temperature T_K is larger than the superconducting pairing energy Δ, a Kondo singlet will form by breaking Cooper pairs at the Fermi level, and then the 0-junction behavior takes place. Instead, the Josephson junction will enter its π phase [7]. Such a result has been predicted theoretically and observed experimentally, by either the sign change of the supercurrent or the crossing behavior of the Andreev bound states [8,9]. As one QD molecule is embedded in the Josephson junction, the spin correlation, Cooper-pair correlation, and the quantum interference mechanisms will take effect simultaneously, which leads to more interesting Josephson phase transition behaviors. For instance, in a T-shaped double-QD junction, an unusual transition occurs in the half-filled case, different from the serially coupled geometry [10–12]. In the Fano-Josephson junction, an intermediate bistable phase has been found to appear in the phase-transition process [13].

With respect to the multi-QD structures, QDs can couple to the leads in a parallel way, in addition to forming the QD molecules. One typical case is the well-known parallel double-QD system, in which the Aharonov-Bohm effect can be observed if local magnetic flux is introduced [14–16]. When the resonant and nonresonant channels are constructed, the Fano effect has an opportunity to govern the quantum transport result [17]. Moreover, in the parallel double-QD system, the strong Coulomb interactions are able to induce the RKKY or SU(4) Kondo effects [18–23].

In view of the special properties of the parallel double-QD system, it is natural to think that they can drive interesting Josephson phase transitions. However, such a topic has not been discussed so far. In this work, we would like to evaluate the Josephson effect in one parallel double-QD junction with two QDs coupled to the superconductors (SCs), respectively. After calculation, we see that the uniformity of the two arms weakens the Josephson phase transition, manifested as the fact that the supercurrent only arrives at its π' phase with the enhancement of the electron correlation. Such a result reflects the special Josephson phase transition characteristics in the parallel double-QD junction.

II. THEORY

The parallel Josephson junction that we consider is illustrated in Fig. 1. Its Hamiltonian is written as $H = H_S + H_{QD} + H_T$. The first term is the Hamiltonian of the SCs within the standard BCS mean-field approximation. It takes the form

$$H_S = \sum_{\alpha k\sigma} \varepsilon_{\alpha k} a^\dagger_{\alpha k\sigma} a_{\alpha k\sigma} + \sum_{\alpha k} (\Delta e^{i\varphi_\alpha} a_{\alpha k\downarrow} a_{\alpha -k\uparrow} + \Delta e^{-i\varphi_\alpha} a^\dagger_{\alpha -k\uparrow} a^\dagger_{\alpha k\downarrow}). \quad (1)$$

φ_α and Δ are superconducting phase and energy gap, respectively, with $\alpha = L, R$. $a^\dagger_{\alpha k\sigma}(a_{\alpha k\sigma})$ is the operator that creates (annihilates) an electron with energy $\varepsilon_{\alpha k}$ for SC-α, where k is the momentum quantum number of the free conduction electrons. Next, H_{QD}, modeling the Hamiltonian for the two QDs, reads

$$H_{QD} = \sum_{j\sigma} \varepsilon_j d^\dagger_{j\sigma} d_{j\sigma} + \sum_j U_j n_{j\uparrow} n_{j\downarrow}. \quad (2)$$

$d^\dagger_{j\sigma}(d_{j\sigma})$ is the operator to create (annihilate) an electron with energy ε_j and spin σ in QD-j ($j = 1, 2$). U_j indicates the strength of intradot Coulomb repulsion in the corresponding

*gwj@mail.neu.edu.cn

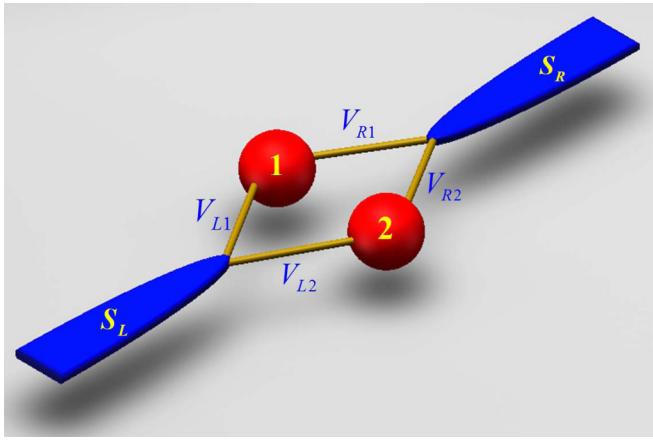

FIG. 1. Schematic of a parallel double-QD Josephson junction. The two QDs connect with two s-wave SCs, respectively.

QD. The last term of H denotes the coupling between the QDs and SCs. For our considered system, it can be directly written as

$$H_T = \sum_{j\alpha k\sigma} (V_{\alpha jk} a^\dagger_{\alpha k\sigma} d_{j\sigma} + \text{H.c.}). \tag{3}$$

$V_{\alpha jk}$ describes the QD-SC coupling coefficient.

It is well known that the phase difference between SCs drives finite current through one Josephson junction. With respect to such a junction, the supercurrent properties can be evaluated by the following formula $I_J = \frac{2e}{\hbar}\frac{\partial\langle H\rangle}{\partial\varphi} = \frac{2e}{\hbar}\frac{\partial\mathcal{F}}{\partial\varphi}$. $\varphi = \varphi_L - \varphi_R$ is the phase difference between the SCs, and $\langle\cdots\rangle$ is the thermal average. Besides, $\mathcal{F}$ is the free energy of the Josephson junction. As one typical case, i.e., zero temperature, $\mathcal{F}$ will be simplified as the ground-state (GS) energy of the system E_{GS}. As a result, the supercurrent can be rewritten as

$$I_J = \frac{2e}{\hbar}\frac{\partial E_{GS}}{\partial\varphi}. \tag{4}$$

Note that in such a structure, the GS determination is a formidable task, which usually requires one appropriate approximation scheme, such as the mean-field approximation and zero-band-width approximation [24,25]. However, in comparison with these methods, the numerical renormalization group (NRG) method is more accurate to reflect the properties of the GS energy [26,27]. We will perform the NRG method to figure out the GS energy. For calculation, we would like to take a few simplifications as follows. The two SCs are assumed to be identical ($\varepsilon_{\alpha k} = \varepsilon_k$ and $\Delta_\alpha = \Delta$) except for a finite phase difference φ. Without loss of generality, we put $\varphi_L = -\varphi_R = \varphi/2$. For the QD-SC coupling, we only consider the case of symmetric junction with $V_{\alpha jk} = V$, so the QD-SC coupling strength can be defined, i.e., $\Gamma = \pi V^2\rho_0$ (ρ_0 is the density of states of the normal states in the SCs). Throughout this work, the QD-SC coupling is fixed at $\Gamma = 0.04\mathscr{D}$ with $\mathscr{D}$ being the width of the conduction band of SC.

The NRG method consists of the following steps. First, the continuum of the conduction band electron states is discretized into intervals of decreasing width as the Fermi level is approached. We linearize the dispersion relation ε_k of the conduction band, which gives $\varepsilon_k = \mathscr{D}k$. Besides, the band Hamiltonian is transformed into the form of a semi-infinite tight-binding chain with the exponentially decreasing hopping constants. As a consequence, the Hamiltonian of the whole system can be written as $\mathcal{H} = \sum_n \mathcal{H}_n$, in which

$$\mathcal{H}_{n+1} = \sqrt{\Lambda}\mathcal{H}_n + \frac{1}{2}(1+\Lambda^{-1})\sum_{l=e,o}\sum_\sigma \xi_n (a^\dagger_{ln\sigma} a_{ln+1,\sigma} + \text{H.c.}) - \Lambda^{n/2}\tilde{\Delta}\sum_{l=e,o} s_l (a^\dagger_{ln+1\uparrow} a^\dagger_{ln+1\downarrow} + \text{H.c.}) \tag{5}$$

with the initial Hamiltonian given by

$$\mathcal{H}_0 = \frac{1}{\sqrt{\Lambda}} H_{QD} + \mathcal{H}_{\tilde{T}} - \Lambda^{n/2}\tilde{\Delta}\sum_{l=e,o}(a^\dagger_{l0\uparrow} a^\dagger_{l0\downarrow} + \text{H.c.}). \tag{6}$$

$$\mathcal{H}_{\tilde{T}} = \sqrt{\frac{2\Gamma}{\pi}}\sum_\sigma \Big[\cos\frac{\varphi}{4}(f^\dagger_{e0\sigma} d_\sigma + \text{H.c.}) - \sin\frac{\varphi}{4}(f^\dagger_{o0\sigma} d_\sigma + \text{H.c.})\Big]. \tag{7}$$

Here the fermion operators $a_{vn\sigma}$ have been introduced as a result of the logarithmic discretization and the accompanying canonical transformation, Λ is the logarithmic discretization parameter (we choose $\Lambda = 2$), $\zeta \sim 1$, and $\mathcal{H}_{QD} \equiv \zeta\frac{H_{QD}}{\mathscr{D}}$, $\tilde{\Delta} = \zeta\frac{\Delta}{\mathscr{D}}$, $V_e = \zeta\sqrt{\frac{2\Gamma}{\pi\mathscr{D}}}\cos\frac{\varphi}{4}$, and $V_o = -\zeta\sqrt{\frac{2\Gamma}{\pi\mathscr{D}}}\sin\frac{\varphi}{4}$, with with $\zeta = 2/(1+1/\Lambda)$. The Hamiltonians $\mathcal{H}_n$ have been rescaled for numerical accuracy. The original Hamiltonian is recovered by $\mathcal{H}/\mathscr{D} = \lim_{n\to\infty}\mathcal{H}_n/\mathcal{J}_n$ with $\mathcal{J}_n = \zeta\Lambda^{(n-1)/2}$. The NRG iterations will be performed until the zero temperature limit is reached and only the lowest-energy part of the spectrum is kept after each iteration step. In our calculations, we keep 1024 states. In order to improve the accuracy of the results, we make use of the interleaved method, also known as z averaging [28,29]. The final results are then calculated as the average over all z parameters.

III. NUMERICAL RESULTS AND DISCUSSIONS

With the help of the above theory, we proceed to evaluate the low-temperature-limit supercurrent in the Josephson junction of parallel double QDs, by assuming identical Coulomb strengths in the QDs, i.e., $U_j = U$. Also, we would like to present the definition of the supercurrent phase for description. If the system's GS energy as a function of φ has a global minimum at the point of $\varphi = 0$ ($\varphi = \pi$), the junction will be located as its 0 (π) phase. For the 0′ (π') phase, it describes the case where one local minimum emerges at the point of $\varphi = \pi$ ($\varphi = 0$) in the E_{GS} spectrum, in addition to the global minimum at $\varphi = 0$ ($\varphi = \pi$) [4].

Before the discussion about the Josephson effect, we would like to concentrate on the renormalization-group (RG) flow of this system. The reason is manifested as the following aspects. The fixed points of the RG flow in QD systems correspond to the respective electronic states, and the electronic states are related to the system's entropy by the formula $\mathcal{S}_{QD} \propto \ln W$. Thus, the entropy change can be utilized to discuss the electronic states of the QDs (i.e., the freezing behaviors of the electrons' degree of freedom). It is known that compared with the ideal Josephson junction without QDs, the contribution of

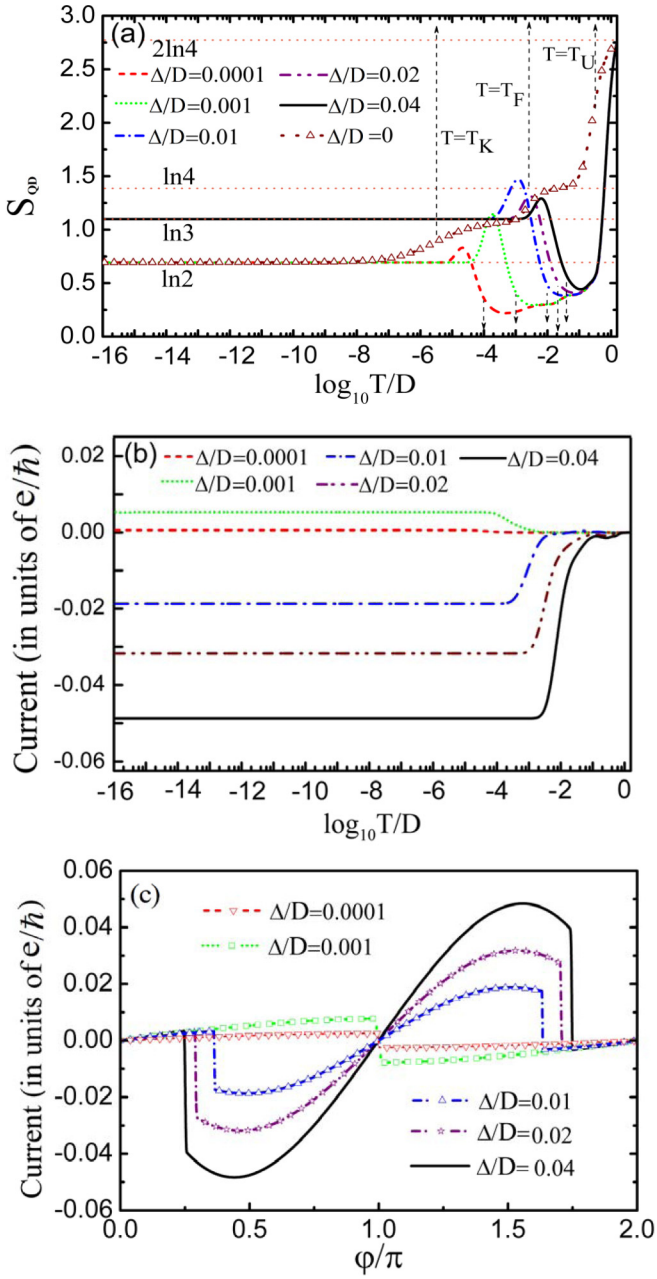

FIG. 2. (a) Temperature dependence of the entropy and (b) the supercurrent in our system calculated by the NRG method. Relevant parameters are taken to be $U/\Gamma = 20$, $\Gamma = 0.04\mathscr{D}$, and $\varphi = \frac{\pi}{2}$, with the bandwidth of SCs $\mathscr{D} = 1$ as the global energy unit. The QD levels are set at the electron-hole symmetry point, i.e., $\varepsilon_j = \varepsilon = -\frac{U}{2}$. (c) Results of supercurrent vs superconducting phase difference φ with the increase of superconducting pairing potential Δ.

QDs to the system's entropy change can be defined as [30]

$$\mathcal{S}_{QD} = \frac{(E-F)}{T} - \frac{(E-F)_0}{T} \tag{8}$$

with $E = \langle H \rangle = \mathrm{Tr}[He^{-H/k_BT}]$ and $F = -k_BT \ln \mathrm{Tr}[e^{-H/k_BT}]$. The subscript 0 denotes the QD-absent situation. The numerical results of $\mathcal{S}_{QD}$ are shown in Fig. 2(a) with $\varepsilon_j = \varepsilon = -\frac{U}{2}$. Here, in order to investigate the effect of the SCs on the Kondo temperature and the RKKY interaction of the double QDs, we first plot the curve of *entropy versus temperature* in the case of the normal metallic leads. It clearly shows that $\mathcal{S}_{QD}$'s magnitude reduces in the stepwise manner, following the decrease of temperature. And then, we can define three transition temperatures to differentiate the characteristic intervals from one another. The first transition temperature is T_U [see Fig. 2(a)]. When the system's temperature exceeds it, the QDs enter the free-orbit regime, in which the four states, i.e., $|0\rangle$, $|\uparrow\rangle$, $|\downarrow\rangle$, and $|\uparrow,\downarrow\rangle$ appear with equal probability. So, 4^2 states exist in the two QDs and the entropy exhibits its value $2\ln 4$. With the NRG iteration, the temperature decreases, and the system reaches the local magnetic-moment regime. Herein, the empty and double-occupied states are both suppressed, while the two single-occupied states appear with equal probability. As a result, the entropy is halved with $\mathcal{S}_{QD} = \ln 4$. Between the temperatures of such two entropy values, T_U can be defined, i.e., $T_U = \frac{1}{2}(T_{S=2\ln 4} + T_{S=\ln 4})$ [30]. As the temperature is further reduced, the QDs are locked into the high-spin states with $S = \frac{N}{2}$ (N is the QD number), due to the RKKY interaction between local spins in the QDs. This is exactly the so-called ferromagnetically frozen regime (FFR). In this case, the entropy decreases further to $\mathcal{S}_{QD} = \ln 3$. Accordingly, the second transition temperature can be ascertained, i.e., $T_F = \frac{1}{2}(T_{S=\ln 4} + T_{S=\ln 3})$. Next, the further decrease of temperature will cause the electrons in the double QDs to be screened by the free electrons in the metallic leads. The QDs enter the partially quenched regime, which is usually referred to as the strong-coupling regime. In this situation, the total spin of the QDs will change from $S = 1$ to $\tilde{S} = S - \frac{1}{2} = \frac{1}{2}$, and the entropy decreases to be $\mathcal{S}_{QD} = \ln(2\tilde{S}+1) = \ln 2$. Accordingly, the third transition temperature can be written out, i.e., $T_K = \frac{1}{2}(T_{S=\ln 2} + T_{S=\ln 3})$, which is the Kondo temperature.

The appearance of three transition temperatures inevitably leads to the complicated Josephson effect in our considered junction. Next, we consider the SCs to couple to the QDs and study the entropy changes by increasing the superconducting paring potential Δ from $\frac{\Delta}{\mathscr{D}} = 10^{-4}$ to $\frac{\Delta}{\mathscr{D}} = 0.04$ [see Fig. 2(a)]. One can find an interesting phenomenon that bordered by the axis of $T_F = 0.0023\mathscr{D}$, the entropy of the system reaches $\ln 2$ when the group flow approaches the fixed point, in the situation of $\Delta < T_F$. Instead, once $\Delta > T_F$, the system's entropy reaches $\ln 3$. As a result, in these two cases, the positive and negative supercurrents come into being, respectively, as shown in Fig. 2(b). Further investigation shows that the supercurrent arrives in two distinct phase regions, i.e., 0 and π' phases [see Fig. 2(c)]. According to the analysis about the transition temperature in the above paragraph, one can find the competitive effect between the Cooper-pairing correlation and ferromagnetic correlation with the increase of Δ. It is such competition that gives rise to the Josephson 0-π' phase transition.

The underlying physics of the phase transition can be described as follows. When Δ is small enough, the fixed point will be located in the strong-coupling regime, as shown by the RG-flow results. The electronic states in the double QDs are dominated by the RKKY ferromagnetic correlation and partial Kondo screening, and the effective spin reduces to be $\tilde{S} = \frac{1}{2}$. It should be noticed that in such a case, Δ is smaller than T_F but much larger than T_K, i.e., $T_K \ll \Delta < T_F$. Surely, though $\Delta >$

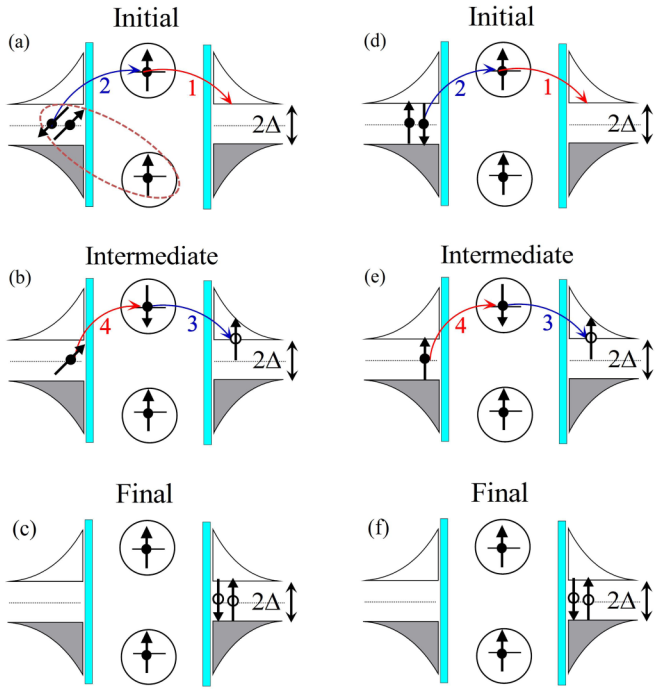

FIG. 3. [(a)–(c)] Illustration of the low-order Cooper-pair tunneling in the 0-junction case with $T_K \ll \Delta < T_F$. [(d)–(f)] The Cooper-pair tunneling in the π'-junction case with $\Delta > T_F > T_K$. The red and blue arrows denote the hopping of electrons with opposite spins, and the numbers (1, 2, 3, and 4) represent the tunneling sequence of electrons.

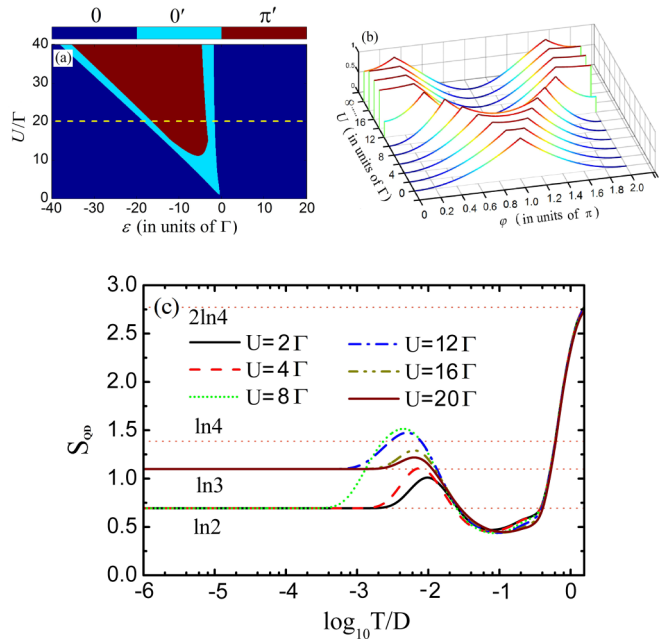

FIG. 4. (a) Phase diagram of the Josephson junction with parallel double QDs. (b) GS level of the junction with the increase of intradot Coulomb strength with $\varepsilon = -\frac{U}{2}$. (c) Temperature dependence of supercurrent when the QD levels are fixed at the electron-hole symmetry point. Parameters: $\varepsilon = -\frac{U}{2}$, $\varphi = \frac{\pi}{2}$, and $\Delta = 0.04\mathscr{D}$.

T_K, no π-junction behavior takes place, completely opposite to the the results in the single-QD junction. The exact reason should be attributed to the appearance of a larger T_F. Thus, it is certain that the 0 phase here originates from the competition among T_F, Δ, and T_K. To be concrete, the dominant energy scale T_F weakens the superconducting-pairing potential Δ and leads to the an effective pairing potential $\tilde{\Delta}$ which is much smaller than T_K. As a consequence, the Cooper pair is broken (interpretively, the Kondo effect survives even in the presence of the SCs), because it aims to screen the localized spins in the QDs to achieve the results of $S = \frac{1}{2}$. Therefore, the final entropy is ln 2, and the Cooper pair can be destroyed easily by the ferromagnetic correlation effect. This exactly gives rise to the sequential-tunneling process shown in Figs. 3(a)–3(c). The ellipse of the dotted line indicates the partially screened effect of electrons in the QDs by the SCs. On the other hand, in the case of $\Delta > T_F > T_K$, the ferromagntic order can be allowed to form in the QDs. However, the Kondo effect can be ignored because the strongly bound Cooper pair cannot be broken. Then, the Cooper pair feels the localized magnetic moment in the QDs. Under this situation, when the Coulomb interaction the QDs is strong enough, the negative-direction supercurrent will appear, which can be clarified with the help of the illustration in Figs. 3(d)–3(f). As shown in Fig. 2(c), the supercurrent is located in the π' phase.

In Fig. 4, we would like to calculate the supercurrent properties in the parallel double-QD junction, by increasing the intradot Coulomb strength. The phase diagram of supercurrent is first shown in Fig. 4(a). One can clearly find that the phase diagram is very similar to the single-QD result, and the phase transition takes place in the region of $-U < \varepsilon < 0$ [4]. However, regardless of the change of the Coulomb interactions or the QD levels, the supercurrent can only arrive at its π' phase, but no π-phase supercurrent comes into being. Such a phase transition can be checked by the result in Fig. 4(b), which describes the GS energy as a function of the intradot Coulomb interaction in the case of $\varepsilon = -\frac{U}{2}$. It shows that with the increase of U, the global minimum of the GS energy moves from the point of $\varphi = 0$ to the position of $\varphi = \pi$. However, in this process, the local minimum of the GS energy always exists at the point of $\varphi = 0$, and it becomes more apparent with the further increase of Coulomb interaction. Therefore, the increase of U cannot modify the $0 \to \pi'$ phase-transition manner in this parallel double-QD junction. This can be explained by the result in Fig. 4(c). It shows that following the increase of U (e.g., from $U = 2\Gamma$ to $U = 20\Gamma$), the entropy value of the double-QD system is only allowed to reach ln 3. This trend is very similar to the phase transition in Fig. 2(a). In fact, at the case of $\varepsilon = -\frac{U}{2}$, in the Kondo regime where $\frac{U}{\Gamma\pi} \gg 1$, the approximate value of the Kondo temperature can be given by Haldane's expression formula [30,31]:

$$T_K = 0.182U\sqrt{\rho_0 J_K}\exp(-1/\rho_0 J_K) \tag{9}$$

with $\rho_0 J_K = 8\Gamma/U\pi$. The temperature of RKKY interaction can be approximated to be $T_F \approx 1.18 J_{RKKY} \sim 1.18U(\rho_0 J_K)^2$. When $U/\Gamma \geqslant 0.4$, there will be $\Delta > T_F > T_K$, so the system will enter the FFR and the π'-junction result arises, like the case in Figs. 2 and 3. It can be readily found that in the case of $\delta = 0$ and $\Delta = 0.04\mathscr{D}$, the increase of U still obeys the energy relationship that $\Delta > T_F > T_K$, and then the

system will be always located in the region of the transition phase π'.

From the discussion on the above results, we can understand the phase transition caused by the three energies, i.e., T_K, Δ, and T_F. On the one hand, in the case of $T_K < \Delta < T_F$, T_F weakens the superconducting pairing potential Δ, and an effective $\tilde{\Delta}$ forms which is much smaller than T_K. This brings about the RKKY-assisted 0-junction behavior, as shown in Figs. 2 and 3(a)–3(c). On the other hand, if $T_K < T_F < \Delta$, the RKKY effect induces the strong ferromagnetic correlation, and then the π phase will be destroyed. Therefore, only the π' phase appears. Even if U increases to infinity, the system has no chance to enter the π phase but only remains at π' phase (mediate phase), which can also be observed in Fig. 4(b). These results indicate that the relation among the three energies is very complicated and that even the "energy cooperation" relation exists between two of them. In order to further understand the double-QD result, we would like to present the results in the single-QD structure, in which the π junction forms in the situation of $T_K \ll \Delta$, only involving the competition between two energy scales. In such a case, the local magnetic moment appears with $S = \frac{1}{2}$ and the fixed point of the system entropy is $\mathcal{S}_{QD} = \ln(2S+1) = \ln 2$. Instead, for our double-QD model, we see in Fig. 4 that the corresponding fixed point of entropy RG flow is $\mathcal{S}_{QD} = \ln(2S+1) = \ln 3$, which corresponds to the strong ferromagnetic order with $S = 1$. After this comparison, one can well understand the phase transition mechanism in the parallel double-QD junction.

In order to further discuss the special Josephson phase transition, we take $\varepsilon_j = \varepsilon$ with $U = 20\Gamma$ and $\varphi = \frac{\pi}{2}$ and plot the spectra of supercurrent, average electron occupation in the QDs, and spin correlations in this junction. The numerical results are displayed in Fig. 5(a)–5(c). The corresponding supercurrent phase is denoted by the dashed line in Fig. 4(a). In Fig. 5(a), one can find that the supercurrent profile is symmetric about the electron-hole symmetry point $\varepsilon = -\frac{U}{2}$, and two peaks appear at the positions of $\varepsilon = 0$ and $\varepsilon = -U$, respectively. For the part of $\varepsilon < -\frac{U}{2}$, it shows that with the increase of the QD levels to the point of $\varepsilon = -20\Gamma$, the supercurrent magnitude reaches its maximum, whereas the following increase first suppresses the current magnitude and then reverses the current direction at the position of $\varepsilon \approx -16\Gamma$. Similarly, when the QD levels increase from the region of $\varepsilon > 0$, a similar process can also be observed.

The supercurrent spectrum in Fig. 5(a) can be clarified with the help of the results in Figs. 5(b) and 5(c). We would like to divide the supercurrent spectrum into five regions according to its variation manner, i.e., regions **A**, **B**, **C**, **D**, and **E**. First, we pay attention to the edge of regions ***A*** and ***B*** where $\varepsilon = -20\Gamma$. At this point, the total electron number in the QDs is equal to 3.0 with $N_\sigma = N_{\bar{\sigma}}$, and the antiferromagnetic correlation between the QD and SCs, namely $\langle \mathbf{S}_L \cdot \mathbf{S}_{1(2)} \rangle$, reaches its maximum. Thus, it is the QD-SC Kondo correlation that magnifies the 0-junction behavior. The underlying physics can be understood as follows. When the QD levels (i.e., $\varepsilon_{1(2)}$) are tuned to the point of $\varepsilon = -20\Gamma$, two opposite-spin electrons are located in the two QDs with their antiferromagnetic correlation. Also, an additional electron occupies the two QDs with equal probability. According to the Pauli exclusion principle, one can know that this electron has no fixed spin orientation. Then, the

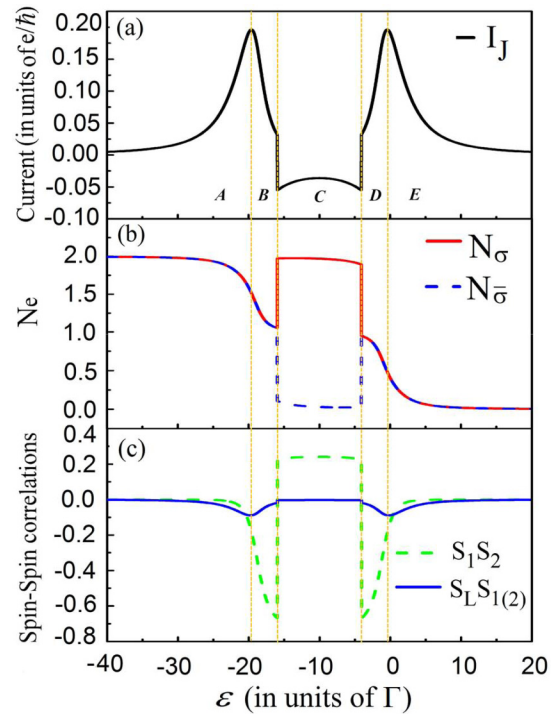

FIG. 5. (a) Spectra of the supercurrent, average electron occupation, and spin-spin correlation of the Josephson junction with parallel double QDs. The system's structural parameters are given as $U = 20\Gamma$ and $\varphi = \frac{\pi}{2}$ with $\varepsilon_j = \varepsilon$.

equal-probability appearance of the opposite-spin states leads to the result that the overall spin of the QDs is $S = 0$. The entropy flow of Fig. 6(a) verifies our analysis. Both of these two cases correspond to the fixed points of the zero-entropy group flow. It shows that the entropy contributed by impurities is equal to zero and impurity spin is completely screened by the Kondo effect. In Figs. 6(b) and 6(c), we present the illustrations of the Cooper pair tunneling mechanism. It can be found that compared with Figs. 3(a)–3(c), their underlying physics are completely different from each other, though they have 0 junctions. In the former case, the entropy flow is ln 2, manifested as the partial Kondo screening, whereas in the latter case the entropy flow of the system is 0 and the QD spin is thoroughly screened by the Kondo effect. We can see that when the QD levels increase from $\varepsilon = -20\Gamma$ to $\varepsilon = -17\Gamma$, the system gets closer to the position of electron-hole symmetry, and the Kondo temperature in the system is reduced [31], so the current gradually decreases. As a result, the supercurrent magnitude is suppressed gradually in region **B**. When the system arrives at the case of $T_K < T_F < \Delta$, it is located at the point of the electron-hole symmetry, the system's entropy flow fixed point is ln 3, the system presents the transition phase π', like the analysis in Fig. 4.

For the result in region **C**, Fig. 5(b) shows that the average electron occupation increases with the decrease of the QD levels, and $N_\sigma = 2.0$ and $N_{\bar{\sigma}} = 0$. The reason consists in the fact that each QD is occupied by one electron and the two electrons possess identical spin orientation. This certainly leads to the ferromagnetic spin correlation between the QDs. As shown in Fig. 5(c), $\langle \mathbf{S}_1 \cdot \mathbf{S}_2 \rangle \approx 0.3$ in such a region. The

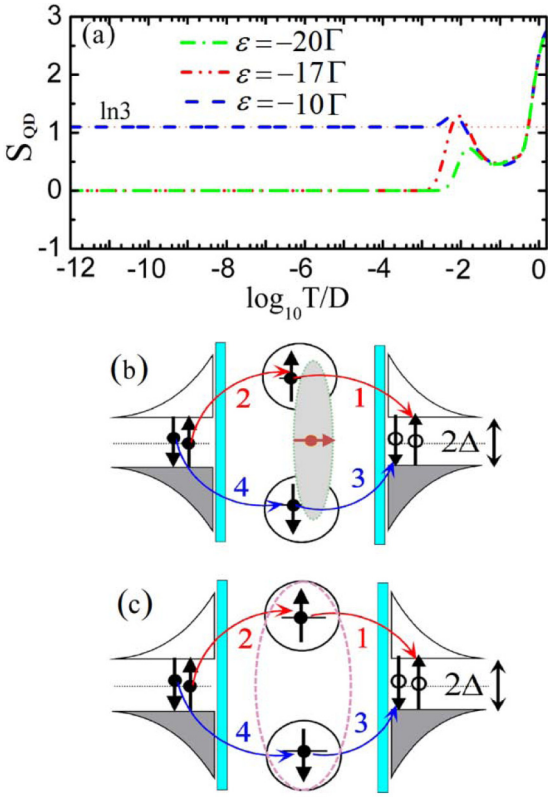

FIG. 6. (a) Entropy of our system calculated by the NRG method with varied the QD levels. (b) Illustrations of the Cooper-pair tunneling in the case of $\varepsilon = -20\Gamma$. (c) Illustrations of the Cooper-pair tunneling in the case of $\varepsilon = -17\Gamma$.

result of $T_K < T_F < \Delta$ is consistent with the former case and the Kondo temperature will be less than the superconducting gap in this region, hence the Cooper-Pair correlation will govern the Josephson effect. Then, the spin ordering of one Cooper pair can be changed during its motion process, which induces the π'-junction behavior [see Figs. 3(d)–3(f)]. It should be noticed that due to the existence of the two identical channels, an electron is allowed to pass through them with the same probability. Accordingly, the nonlocal motion of the electrons in one Cooper pair weakens the π-junction behavior but only leads to the occurrence of the π'-phase supercurrent.

The supercurrent in regions **D** and **E** is similar to that in regions **B** and **A**, respectively. The physics picture can be described by changing electron to hole. At a matter of fact, here one can view the parallel double QDs to be one large $\mathcal{QD}$ by considering the two arms as the pseudospin indexes. Surely, the identity of two arms gives rise to the degeneracy of pseudospin states. One can then find that such a $\mathcal{QD}$ is singly occupied at the case of $\varepsilon = 0$, which drives the occurrence of the Kondo effect. According to the previous works, this is exactly the orbital-Kondo effect. Therefore, the enhanced orbital-Kondo correlation magnifies the Josephson effect. Next, when the QD levels increase, the number of electrons in the QDs decreases, and the additional electron that appears in the "large $\mathcal{QD}$" disappears, leading to two electrons in the QDs which will form the stable antiferromagnetic correlation.

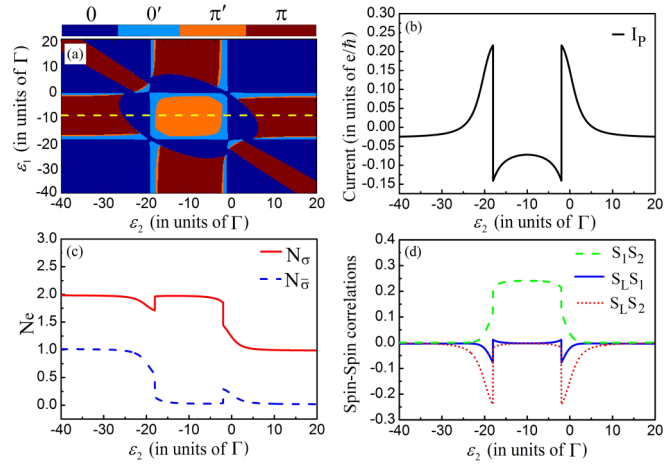

FIG. 7. (a) Influence of detuning the QD levels on the phase diagram of the Josephson junction with parallel double QDs. The system's Coulomb strength is taken to be $U = 20\Gamma$ with $\Gamma = 0.04\mathscr{D}$. [(b)–(d)] Spectra of the supercurrent, average electron occupation, and spin-spin correlation in the case of $\varepsilon_1 = -\frac{U}{2}$ with $\varphi = \frac{\pi}{2}$.

In Fig. 7, we take $U = 20\Gamma$ and detune the QD levels to further present the supercurrent characteristics. The phase diagram is shown in Fig. 7(a). One can clearly observe that this phase diagram exhibits an isolated island of the π'-phase region, bounded by the lines of $\varepsilon_{1(2)} = 0$ and $\varepsilon_{1(2)} = -U$. Outside this island, it is one circular 0-phase region. Next, with the further detuning of the QD levels, the π-junction behavior has an opportunity to appear under the situations of $\varepsilon_j \ll -U$ or $\varepsilon_j \gg 0$, while $\varepsilon_{j'}$ shifts around the electron-hole symmetry point (i.e., $-U < \varepsilon_{j'} < 0$). In our considered junction, such a phenomenon originates from the fact that only one arm contributes to the Cooper-pair tunneling. In recent years, the appearance of the isolated island region and the largely suppressed π phase have become interesting in the aspect of the Josephson effect modified by the electron correlation mechanism [12]. One can then ascertain that the result in Fig. 7(a) provides new information for understanding the isolated island behavior of the phase transition.

We next would like to perform a detailed analysis about the isolated island behavior and then focus on the dashed line shown in Fig. 7(a) to analyze the supercurrent properties in different regions. Figures 7(b)–7(d) show the spectra of supercurrent, average electron occupation, and spin-spin correlations, respectively. For the QD levels, we take one typical case, where $\varepsilon_1 = -10\Gamma$ (i.e., $\varepsilon_1 = -\frac{U}{2}$). It shows that when ε_2 decreases from 20Γ to 5Γ, the supercurrent direction changes smoothly, and hence the direct $\pi \to 0$ phase transition comes into being. Next, in the case of $\varepsilon_2 = -2.0\Gamma$, the positive supercurrent reaches its maximum. Meanwhile, both the direction and magnitude of the supercurrent undergo their sharp change at this position. As a consequence, the Josephson junction enters its π' phase. These results can be explained as follows. The decrease of ε_2 causes its-embedded arm to contribute to the Cooper-pair tunneling. To be specific, this leads to 0-phase supercurrent as a result of the weak electron correlation. The enhancement of such supercurrent gives rise to the direct $\pi \to 0$ phase transition process. Next, when ε_2 decreases below the

system's Fermi level, an electron has a chance to enter QD 2. Accordingly, the Kondo correlation between QD 2 and SCs will affect the Josephson phase transition [see Figs. 7(c) and 7(d)]. Note that in such a case, the Kondo correlation also exists in the arm with QD 1. This conclusion can be made from the results of spin-spin correlations between the QDs and SCs. As shown in Fig. 7(d), $\langle \mathbf{S}_L \cdot \mathbf{S}_1 \rangle$ and $\langle \mathbf{S}_L \cdot \mathbf{S}_2 \rangle$ are all antiferromagnetic in the case of $\varepsilon_2 = -2.0\Gamma$. The interplay between the two Kondo correlations has an opportunity to induce the RKKY effect, which can be viewed as the reason for the $0'$-phase supercurrent. As the level of QD 2 further decreases (i.e., $\varepsilon_2 < -2.0\Gamma$), its spin occupation will become robust, similar to QD 1. Then, the π'-phase behavior comes into play, accompanied by the enhancement of the RKKY effect.

IV. SUMMARY

In summary, we have presented an analysis about the Josephson phase transition in a parallel junction in which each arm has one embedded QD. It has been found that if the two QDs are half-occupied, the Josephson phase transition will become weak. To be concrete, with the enhancement of the electron correlation, the supercurrent can only arrive at its π' phase but does not enter its π phase. We consider such a result to be caused by the interplay among the Kondo, RKKY, and Cooper-pairing correlations. Next, the isolated island behavior has been observed when the QD levels are detuned. Based on the obtained results, we believe that this work can be helpful in understanding the Josephson phase transition modified by interaction between the electron correlations and Cooper-pairing mechanism.

ACKNOWLEDGMENTS

This work was financially supported by the Fundamental Research Funds for the Central Universities (Grants No. N160504009 and No. N170506007) and the National Natural Science Foundation of China (Grant No. 11604221). Our numerical results are obtained via NRG LJUBLJANA open-source numerical renormalization group code.

[1] Y. Meir, N. S. Wingreen, and P. A. Lee, Phys. Rev. Lett. **70**, 2601 (1993).
[2] D. Goldhaber-Gordon, J. Göres, M. A. Kastner, H. Shtrikman, D. Mahalu, and U. Meirav, Phys. Rev. Lett. **81**, 5225 (1998).
[3] S. M. Cronenwett, T. H. Oosterkamp, and L. P. Kouwenhoven, Science **281**, 540 (1998).
[4] A. V. Rozhkov and D. P. Arovas, Phys. Rev. Lett. **82**, 2788 (1999).
[5] C. Buizert, A. Oiwa, K. Shibata, K. Hirakawa, and S. Tarucha, Phys. Rev. Lett. **99**, 136806 (2007).
[6] J.-P. Cleuziou, W. Wernsdorfer, V. Bouchiat, T. Ondarçuhu, and M. Monthioux, Nat. Nanotech. **1**, 53 (2006).
[7] G. Sellier, T. Kopp, J. Kroha, and Y. S. Barash, Phys. Rev. B **72**, 174502 (2005).
[8] E. Vecino, A. Martín-Rodero, and A. Levy Yeyati, Phys. Rev. B **68**, 035105 (2003).
[9] J. A. van Dam, Y. V. Nazarov, E. P. Bakkers, and S. De Franceschi, Nature (London) **442**, 667 (2006).
[10] G. Yi, L. An, W. J. Gong, H. Wu, and X. Chen, Phys. Lett. A **377**, 1127 (2013).
[11] F. S. Bergeret, A. Levy Yeyati, and A. Martín-Rodero, Phys. Rev. B **74**, 132505 (2006).
[12] R. Žitko, M. Lee, R. López, R. Aguado, and M. S. Choi, Phys. Rev. Lett. **105**, 116803 (2010).
[13] G. Yi, Z. Li, X. Chen, H. Wu, and W. J. Gong, Phys. Rev. B **87**, 195442 (2013).
[14] Z. Wang and X. Hu, Phys. Rev. Lett. **106**, 037002 (2011).
[15] R. Žitko and J. Bonča, Phys. Rev. B **76**, 241305(R) (2007).
[16] T. Hatano, T. Kubo, Y. Tokura, S. Amaha, S. Teraoka, and S. Tarucha, Phys. Rev. Lett. **106**, 076801 (2011).
[17] A. E. Miroshnichenko, S. Flach, and Y. S. Kivshar, Rev. Mod. Phys. **82**, 2257 (2010).
[18] R. Žitko, J. Mravlje, and K. Haule, Phys. Rev. Lett. **108**, 066602 (2012).
[19] A. L. Chudnovskiy, Europhys. Lett. **71**, 672 (2005).
[20] C. A. Bŭsser, A. E. Feiguin, and G. B. Martins, Phys. Rev. B **85**, 241310(R) (2012).
[21] D. Krychowski and S. Lipiński, Phys. Rev. B **93**, 075416 (2016).
[22] K. Wrześniewski and I. Weymann, Phys. Rev. B **96**, 195409 (2017).
[23] A. J. Keller, S. Amasha, I. Weymann, C. P. Moca, I. G. Rau, J. A. Katine, H. Shtrikman, G. Zaránd, and D. Goldhaber-Gordon, Nat. Phys. **10**, 145 (2014).
[24] F. S. Bergeret, A. Levy Yeyati, and A. Martín-Rodero, Phys. Rev. B **76**, 174510 (2007).
[25] R. Allub, Phys. Rev. B **67**, 144416 (2003).
[26] J. Bauer, A. Oguri, and A. C. Hewson, J. Phys.: Condens. Matter **19**, 486211 (2007).
[27] J. S. Lim and M. S. Choi, J. Phys.: Condens. Matter **20**, 415225 (2008).
[28] R. Žitko, O. Bodensiek, and T. Pruschke, Phys. Rev. B **83**, 054512 (2011).
[29] R. Žitko and J. Bonča, Phys. Rev. B **77**, 245112 (2008).
[30] R. Žitko and J. Bonča, Phys. Rev. B **74**, 045312 (2006).
[31] R. Žitko and J. Bonča, Phys. Rev. B **73**, 035332 (2006).